J. Fluid Mech. (1986), *vol.* 162, *pp.* 157–170
Printed in Great Britain

The sedimentation of one sphere past a second attached to a wall

By K. MAŁYSA†, T. DĄBROŚ‡ AND T. G. M. VAN DE VEN

Pulp and Paper Research Institute of Canada and Department of Chemistry, McGill University, Montreal, Quebec, Canada, H3A 2A7

(Received 27 January 1984 and in revised form 17 June 1985)

Experimental results are reported on hydrodynamic interactions between a solid plate with a spherical particle attached to it and a rigid sphere moving parallel to the plate. Trajectories and velocities of the moving sphere were determined by taking single-frame multiple-image photographs using stroboscopic light.

Sphere–sphere hydrodynamic interactions were detectable on the background of plate–sphere interactions for initial dimensionless sphere–wall separations $Z_0 < 4.9$. The sphere trajectories were found to be symmetrical for $Z_0 \geqslant 2.3$ and asymmetrical otherwise. For asymmetrical trajectories the sphere velocity was larger after the encounter than prior to it. It was concluded that surface roughness of the spheres was responsible for the observed deviations from symmetry.

Numerical calculations were performed to obtain sphere trajectories and velocities. The calculations agree with the experimental data for dimensionless distances between sphere centres $r > 2.5$. For $r < 2.5$ the numerical results were in fair agreement with the data when $Z_0 \gtrsim 2.9$. For smaller Z_0, theoretical predictions were inaccurate.

1. Introduction

After a decade of rather intense theoretical and experimental efforts hydrodynamic interactions between two spheres in Newtonian low-Reynolds-number flow are by now well understood, both in the presence and absence of external (gravity, electric and magnetic fields, etc.) or internal forces (van der Waals, double-layer interactions, etc.), (Batchelor & Green 1972; Arp & Mason 1977*a*, *b*; van de Ven & Mason 1976, 1977; Adler 1981*a*,*b*; Takamura, Goldsmith & Mason 1981; van de Ven 1982; Jeffrey & Onishi 1984). All these efforts were directed to two-sphere systems in unbounded liquids in which the influence of neighbouring walls was neglected. In many practical applications wall effects can be of tremendous importance, especially in problems related to surface aggregation and coating. For instance, it is well known that the presence of particles on a surface strongly affects the rate at which particles deposit on collector surfaces. Particles deposited on a surface are sometimes able to block (making unavailable for further deposition) an area 25 times their size (Dąbroś & van de Ven 1982, 1983). It is believed that in two-particle collisions at a wall a mobile sphere can be pushed away from the wall by a deposited sphere, thus reducing its probability of deposition.

The influence of a wall on a single sphere is also well understood (Faxen 1923;

† On leave from the Polish Academy of Sciences, Krakow, Poland.

‡ Present address: Department of Physical Chemistry and Electrochemistry, Jagiellonian University, Krakow, Poland.

Goldman, Cox & Brenner 1967; O'Neill & Stewartson 1967; O'Neill 1968; Cox & Mason 1971). Experimental verifications of several aspects of sphere–wall interactions have been published as well (Darabaner & Mason 1967; Miyamura, Jwasaki & Ishii 1981; Ambari, Manuel & Guyon 1983; Adamczyk, Adamczyk & van de Ven 1983), but agreement for very short sphere–wall separations is usually poor.

This paper deals with two-sphere interactions near a wall, one of the spheres being immobile and attached to the wall, the other one being freely mobile. Approximate theories are developed to describe these interactions. Experiments are described for determining the trajectories and velocities of the mobile sphere and the results are compared with theory.

2. Theory

Let us consider two spherical particles subjected to gravity in the proximity of a solid wall in an incompressible fluid satisfying the stationary creeping-flow equation

$$\mu \nabla^2 \boldsymbol{v} = \boldsymbol{\nabla} p, \tag{1}$$

$$\boldsymbol{\nabla} \cdot \boldsymbol{v} = 0, \tag{2}$$

where $\boldsymbol{v} = (v_x, v_y, v_z)$ is the fluid-velocity vector, p the pressure and μ the dynamic viscosity. The Cartesian coordinate system will be oriented in such a way that the wall coincides with the $z = 0$ plane and the gravitational force acts in the y-direction. A schematic representation is given in figure 1. We want to calculate the velocity of particle A which is free to move and to rotate. Particle B is kept stationary at a given position by external forces F_x^B, F_y^B, and F_z^B which will counteract the hydrodynamic forces produced by the flow disturbances caused by particle A. The settling velocity of particle A is affected by the presence of particle B and the wall. An external force acting upon A is at any instant, through viscous stresses, transferred to the fluid, producing flow disturbances which in turn must satisfy the no-slip boundary condition at the surfaces of particles and wall and tend to zero at infinity. To obtain the solution of this problem, which is well-defined and possesses a unique solution, we can make use of the singularity method, described by Dąbroś (1985).

Generally speaking, in this method one looks for such intensities of the singular forces and sources located near the particle's centre, and eventually for such translational and angular velocities of the given particle, that the no-slip boundary conditions are satisfied, at least in a least-mean-square sense, at the particle's surfaces. When a particle is free to translate and rotate, the sum of the proper components of the singular forces in each particle, and the torques associated with them, must be equal to the external force and torque acting upon the particle. This requirement yields a number of constrained equations imposed on the singular forces of every particle which must be satisfied exactly.

The flow velocity v_i at (x_1, y_1, z_1) produced by a point force f_j acting at (x_2, y_2, z_2) in the presence of a solid-plane wall located at $z = 0$ is given by (Blake 1971; Blake & Chwang 1974):

$$v_i(x_1, y_1, z_1) = \frac{1}{8\pi\mu}(t_{ij} + t_{ij}^*) f_j. \tag{3}$$

Here t_{ij} is the Oseen tensor

$$t_{ij} = \frac{\delta_{ij}}{r} + \frac{r_i r_j}{r^3}, \tag{4}$$

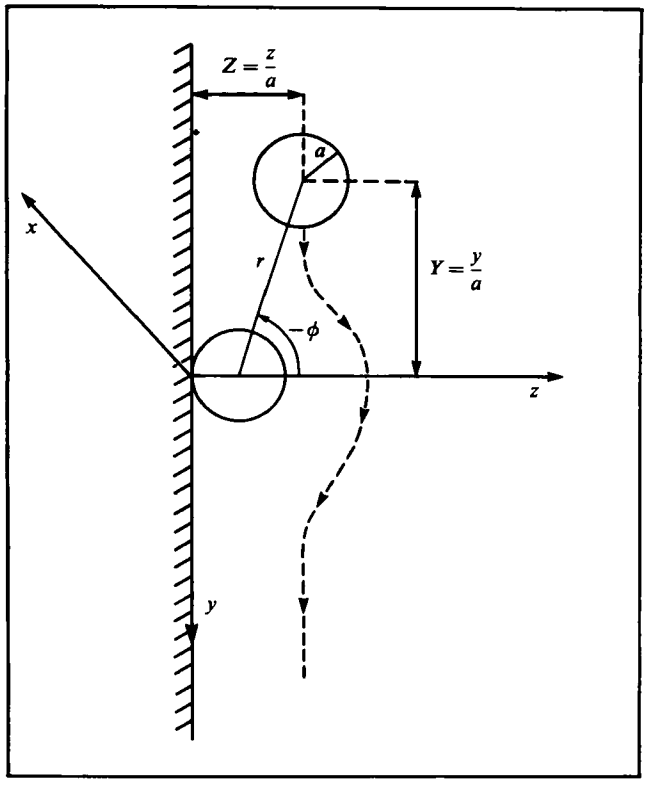

FIGURE 1. Coordinates and notations used in the description of the system.

where $r_1 = x_1 - x_2, r_2 = y_1 - y_2, r_3 = z_1 - z_2$ and $r = (\Sigma r_i^2)^{\frac{1}{2}}$. The second term in brackets in (3) can be related to the image system, in this case consisting of a Stokeslet (point force), a Stokes doublet and a source doublet with a proper strength to make the fluid velocity equal to zero at $z = 0$. Blake has shown that

$$t_{ij}^* = -\left(\frac{\delta_{ij}}{R} + \frac{R_i R_j}{R^3}\right) + 2z_2(\delta_{j\alpha}\delta_{\alpha k} - \delta_{j3}\delta_{3k})\frac{\partial}{\partial R_k}\left[\frac{z_2 R_i}{R^3} - \left(\frac{\delta_{i3}}{R} + \frac{R_i R_3}{R^3}\right)\right], \tag{5}$$

where $\alpha = 1, 2; R_1 = x_1 - x_2, R_2 = y_1 - y_2, R_3 = z_1 + z_2$ and $R = (\Sigma R_i^2)^{\frac{1}{2}}$. The disturbance flow at (x_1, y_2, z_1) caused by a singular source at (x_2, y_2, z_2) with volume outflow M per unit time, equals

$$u_i = \frac{M}{4\pi} s_i, \tag{6}$$

where, in the presence of a stationary-plane boundary at $z = 0$, s_i is given by

$$s_i = \left(\frac{r_i}{r^3} - \frac{R_i}{R^3}\right) - 2\left(\frac{R_i}{R^3} - \frac{3R_i R_j R_3}{R^5}\right) + 2z_2\left(\frac{\delta_{i3}}{R^3} - \frac{3R_i R_3}{R^5}\right). \tag{7}$$

In the calculations of the velocity of the free sphere, we have used 13 singular forces and sources distributed symmetrically at $(0, 0, 0)$, $(\pm b, 0, 0)$, $(0, \pm b, 0)$ and $(0, 0, \pm b)$ with $b = 0.01$ and 0.1 (b non-dimensionalized by the sphere radius). The number of surface points (to define the shape of the particle) was equal to 42. These points too were distributed symmetrically over the surface of the sphere. An identical number

and distribution of singular forces and sources and surface points were used for the stationary sphere. For the stationary sphere, the velocity of the surface points is equal to zero, and no constraints are placed on the intensities of the singularities. The mobile sphere was free to rotate and translate under gravity forces. The sum of the appropriate components of the singular forces must be balanced against those of the external forces. Because no external torque is imposed on the particle, the singular forces must fulfil the condition that the torque caused by them equals zero.

When the mobile sphere is close to the immobile one, this method becomes inaccurate. In principle the accuracy can be improved by taking more singular forces and sources. For more details the reader is referred to the paper by Dąbroś (1985). This singularity method was used to calculate the velocity of the freely mobile spheres, which is compared with the experimental velocities described below in §3.

It is of interest to look at the limit of the gap width ϵ between the spheres approaching zero. For such conditions the singularity method outlined above fails. As $\epsilon \to 0$, the trajectory becomes identical with that of a freely mobile sphere to a fixed one in the absence of a wall, the forces and torques being dictated by the lubrication in the gap. Assume the fixed sphere at the centre of a polar coordinate system (r, ϕ), r being the dimensionless centre-to-centre distance and ϕ the angle between the z-axis and r; then the forces F and torque T on the freely mobile sphere can be expressed as:

$$F_r = c_1 u_r = mg \sin\phi, \tag{8a}$$

$$F_\phi = c_2 u - c_3 \omega = mg \cos\phi, \tag{8b}$$

$$T = -c_3 u_\phi + c_4 \omega = 0. \tag{8c}$$

Here $u_r = \mathrm{d}r/\mathrm{d}t$, $u_\phi = r\,\mathrm{d}\phi/\mathrm{d}t$ and ω is the angular velocity of the free sphere. For equal spheres (Stimson & Jeffery 1926; Maude 1961; Davis 1969; O'Neill & Majumdar 1970; Jeffrey & Onishi 1984):

$$c_1 = \frac{3\pi\mu a}{2\epsilon}, \qquad c_2 = -\pi\mu a \ln\epsilon,$$

$$c_3 = \pi\mu a^2 \ln\epsilon, \quad c_4 = -\tfrac{8}{5}\pi\mu a^3 \ln\epsilon.$$

From (8) it follows that

$$\frac{u_r}{u_\phi} = \frac{\mathrm{d}r}{\mathrm{d}\phi} = \frac{c_2 c_4 - c_3^2}{c_1 c_4} \tan\phi. \tag{9}$$

Integration of (9) yields the trajectory equation

$$\cos\phi = \left(\frac{\ln\epsilon}{\ln\epsilon_m}\right)^2, \tag{10}$$

ϵ_m being the minimum gap width when $\phi = 0$. It can be seen that the trajectories are symmetrical with respect to $\phi = 0$. This is not only true for small gap widths ϵ, but for all trajectories, a fact which follows directly from the linearity of the creeping-flow equation.

Comparison of the trajectory of a freely mobile sphere in the presence of a wall with that in the absence of a wall is useful in determining a lower limit of the gap width between the two spheres. When $\phi = 0$ and for a given gap width, in the absence of a wall the velocity $u_{\phi=0}$ (the velocity u_ϕ at $\phi = 0$) is higher than in the presence of the wall, because with the wall the hydrodynamic resistance is increased. It follows that for a given sphere velocity the gap between the spheres will be larger in the

presence of the wall than in its absence. From the values of the coefficients c_i in the absence of a wall it can be shown that

$$\frac{u_{\phi=0}}{u_\infty} = \frac{-16\ln\epsilon + 56.224}{\ln^2\epsilon - 28.531\ln\epsilon + 54.605}, \tag{11}$$

where u_∞ is the velocity of a single sphere in an unbounded fluid.

3. Experimental

The experiments consisted of observing, filming and analysing the motion of a sphere falling parallel to a transparent wall to which a second sphere was attached.

The experiments were carried out using the single-frame multiple-image technique. The essential parts of the experimental set-up were the same as described elsewhere (Adamczyk, Adamczyk & van de Ven 1983). It consisted of a Plexiglas reservoir of dimensions $42 \times 42 \times 52$ cm with two viewing windows (14×29 cm) made of high-quality optical glass, and two perpendicularly located Linhoff photo cameras.

A nylon sphere of diameter 0.6357 ± 0.0008 cm was glued to the centre of a Plexiglas plate of size 30×35 cm. The plate was mounted perpendicularly to a base plate equipped with adjustable screws, allowing for a precise vertical position. The whole element was subsequently located inside the reservoir in such a manner that the vertical Plexiglas plate was in the median plane of the reservoir, with the fixed sphere at its centre. The optical axis of one camera was perpendicular, and of the other camera parallel, to the plate with the sphere. Both cameras and the reservoir could be moved up and down within a 30 cm range. A stroboscopic lighting system was used to illuminate the experimental set-up. The flashing light source was triggered externally with the help of a Contax RTS II quartz photo apparatus having a professional motor drive. This drive is equipped with a built-in interval timer which allows one to trigger the stroboscopic lamp with a preset frequency. By taking photographs of a stop-watch, it was found that the uncertainty of the timer was about 0.5–1.0%.

The reservoir was filled with a silicone oil (Dow Corning) of density 0.9735 g/cm^3 and kinematic viscosity of 9.82 stokes (25 °C). A nylon sphere with diameter of 0.6362 ± 0.0011 cm was used as the moving sphere. The size of the spheres was measured using a Nikon shadograph. Twenty measurements of the sphere diameter were made at different positions and the average value was calculated. At the beginning of each experiment, the free sphere was sucked, with the help of a water pump, to the tip of a pipette which was maintained in a special holder equipped with two screws, allowing motion in two perpendicular directions within a distance of a few centimetres. The tip of the pipette was positioned a few millimetres below the oil surface. The pipette with the sphere was placed at a chosen distance from the Plexiglas plate and subsequently the sphere was released by switching off the suction. The Linhoff camera with optical axis perpendicular to the plate with the attached sphere, was used to check if the falling sphere was in the equatorial (y, z)-plane of the attached sphere. The pipette was moved parallel to the plate until the images of the moving sphere covered the image of the fixed one. Polaroid High Speed (9×12 cm) Land Film Type 57 was used to take the multiple-image photographs of the moving sphere. An example of photographs from both cameras is presented in figure 2. Photographs from the camera with optical axis parallel to the plane were used to determine the sphere velocity and its trajectory near the attached particle.

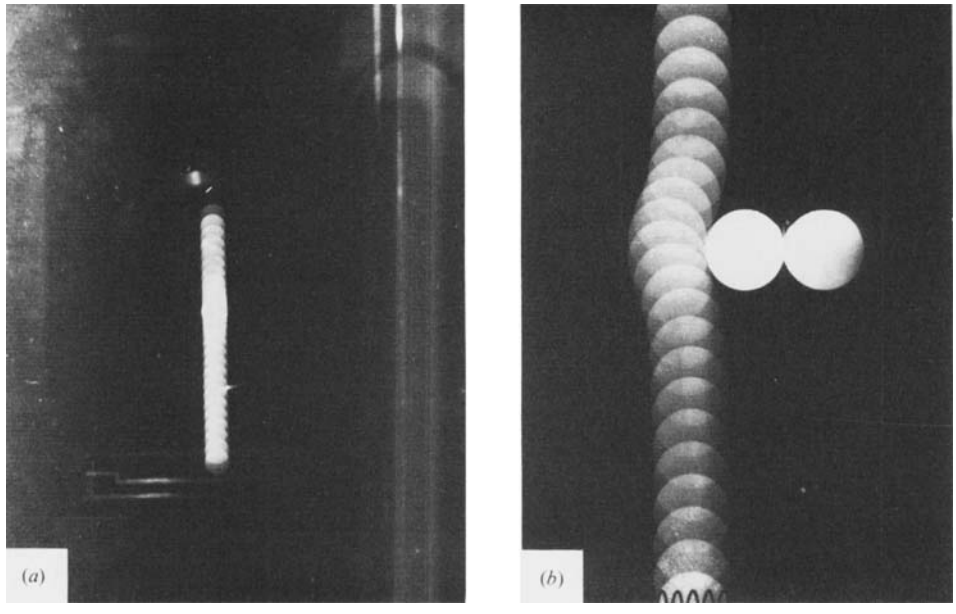

FIGURE 2. Photographs obtained by multiple image technique from the camera with optical axis (*a*) perpendicular, (*b*) parallel, to the plate with attached sphere.

The positions of the sphere images in the photographs were measured with a precision of 0.01 mm.

For each experimental run the cameras were fixed at three different positions: above, at the same level as, and below, the attached particle. Thus, the motion of the free sphere could be detected both before and after the encounter with the attached particle. All experiments were performed at a temperature of 25 ± 0.2 °C. The Reynolds number based on the sphere diameter was 10^{-2}, so that the conditions of creeping flow applied.

The radius a and the coordinates y and z of the centre (see figures 1 and 2) of the moving sphere were measured in each photograph. At a given position of the sphere its velocity in the y-direction can be expressed, in units normalized with respect to the sphere radius, as

$$u_y = \frac{Y_{(i+1)} - Y_{(i-1)}}{2\Delta t} \quad [\text{units of radius s}^{-1}], \tag{12}$$

where i refers to the frame number and Δt the time between flashes.
Analogously we have

$$u_z = \frac{Z_{(i+1)} - Z_{(i-1)}}{2\Delta t} \quad [\text{units of radius s}^{-1}]. \tag{13}$$

The total particle velocity $\boldsymbol{u}$ is equal to the vectorial sum of its component in both y- and z-directions:

$$\boldsymbol{u} = \boldsymbol{u}_y + \boldsymbol{u}_z, \quad \boldsymbol{u}_x = 0. \tag{14}$$

We define a normalized velocity of the particle near the wall as $\boldsymbol{U} = \boldsymbol{u}/u_\infty$. The normalized velocities were calculated from the particle velocity which was determined experimentally in the centre of the reservoir after removing the plate with the attached particle. The determined u_∞-value was equal to 0.991 ± 0.014 radius s^{-1} (average from three independent experimental runs). The ratio of the radius of the

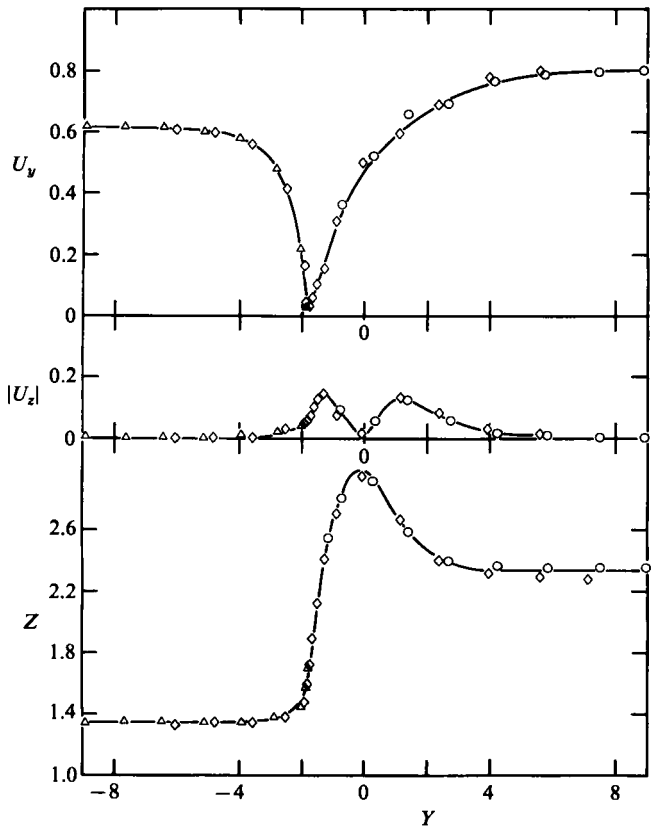

FIGURE 3. The y- and z-components of the sphere velocity, and its trajectory as a function of the dimensionless distance Y from the centre of attached particle for initial separation $Z_0 = 1.34$. Symbols refer to various experimental runs. Lines are smooth fits through the data.

moving sphere and the distance to the wall was 0.015. The experimentally determined u_∞-value was about 3.5% lower than the theoretical value for an unbounded fluid ($mg/6\pi\mu a$). From the experimental data on correction factors in square cylinders by Miyamura, Jwasaki & Ishii (1981), it can be concluded that this difference is solely due to wall interactions. For convenience, our experimental results are normalized with respect to experimentally determined u_∞-values.

4. Results and discussion

The trajectories and sphere velocities for initial separations close to the wall are given in figure 3 and for initial separations relatively far from the wall in figure 4. Both figures show the y- and z-components of the sphere velocity ($u_x = 0$) and the sphere trajectory (z *vs.* y). For figure 3, the initial separation to the wall $Z_0 (= z/a) = 1.34$ while, for figure 4, $Z_0 = 2.88$. It can be seen that for small separations the trajectories and velocities are asymmetric, while for large separations they become symmetric. When $Y (= y/a) < -6$ or $Y > 6$, the particle velocity in the y-direction is approximately constant and in the z-direction approximately zero. For these orientations the particles move parallel to the wall (z is constant). Closer to the sphere U_y decreases and reaches a minimum. For symmetrical trajectories a wide

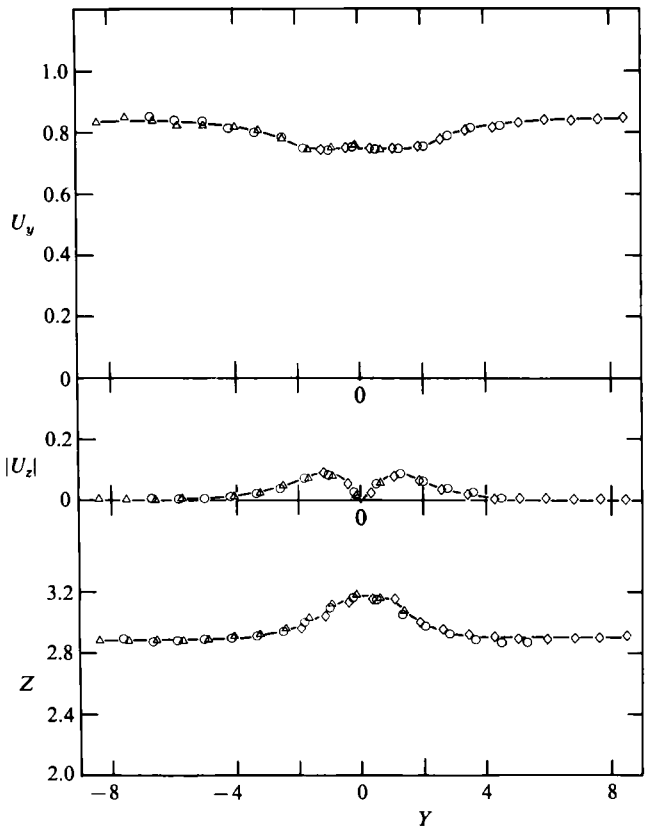

FIGURE 4. The y- and z-components of the sphere velocity, and its trajectory as a function of dimensionless distance Y from the centre of attached particle, for initial separation $Z_0 = 2.88$. Symbols refer to various experimental runs. Lines are smooth fits through the data.

shallow minimum occurs around $Y = 0$, while for asymmetric trajectories a steep minimum occurs for $Y < 0$. The steepness of the minimum decreases with increasing Z_0. $|U_z|$ shows two maxima located symmetrically about $Y = 0$, which are slightly asymmetric for small Z_0-values ($U_z < 0$ for $Y > 0$). For the trajectory in figure 3 (Z *vs.* Y curve) it can be seen that for low Z_0 the distance to the wall of the mobile sphere is larger after the encounter than prior to it. This larger distance corresponds to a higher velocity after the encounter. For $Z_0 \geqslant 2.3$ trajectories and velocities were found to be symmetric.

The particle velocity $U = |U|$ is shown in figures 5 and 6 as a function of the dimensionless distance Y for the investigated range of initial separation distances Z_0 together with numerical results of the singularity methods (solid lines). The numerical data start to deviate from the experimental data for small values of Y ($-2 < Y < 2$), i.e. when the systems are close together. For $Z_0 \geqslant 4.9$ (figure 5), no hydrodynamic interactions between the fixed and free spheres were detected on the background of interactions with the plate. For the interaction between the mobile and a fixed sphere in the absence of a wall, the deviation from a straight trajectory is predicted to be 5% for $Z_0 = 4.9$, but in the presence of a wall the deviation will be different. Within the range $2.3 \leqslant Z_0 < 4.9$ (figure 5), the particle motion was practically symmetrical about the z-axis. The velocities of the moving sphere were identical before and after

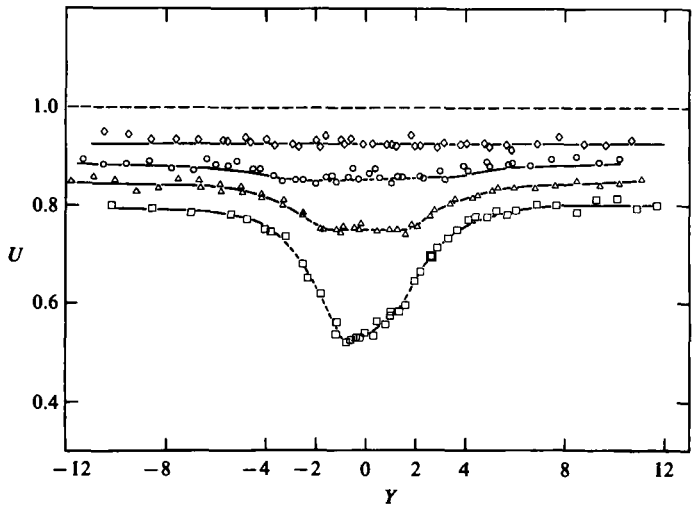

FIGURE 5. The total sphere velocity U as a function of dimensionless distance Y for various initial separations $Z_0 > 2.0$. ◇, $Z_0 = 4.90$; ○, $Z_0 = 3.57$; △, $Z_0 = 2.88$; □, $Z_0 = 2.34$. The solid parts of the lines are calculated numerically, using the singularity method. For short separations $|Y| \leqslant 3$, this method becomes inaccurate. Dashed posrtions are smooth fits through the data.

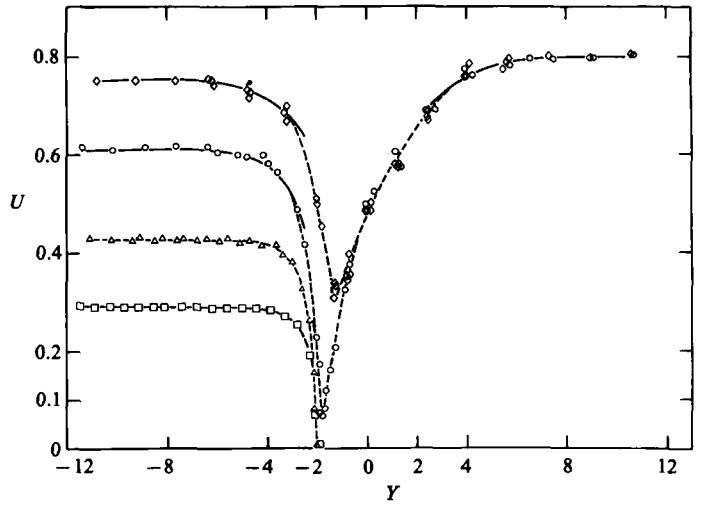

FIGURE 6. The total sphere velocity U as a function of dimensionless distance Y for various initial separations $Z_0 \leqslant 2.0$. ◇, $Z_0 = 2.00$; ○, $Z_0 = 1.35$; △, $Z_0 = 1.05$; and, □, $Z_0 < 1.01$ (sphere pressed against plate). Solid parts of curves ($|Y| > 2.5$) are calculated from the singularity method. Dashed parts are smooth experimental fits.

the encounter, i.e. for $Y < -2$ and $Y > 2$. Near the attached particle, i.e. for $-2 < Y < 2$, the velocity of the sphere was minimum. When the initial separation distances $Z_0 \geqslant 2.3$ this minimum was not sharp, but a rather large region of nearly constant velocity near the fixed particle was observed. When $Z_0 \lesssim 2$, minima in U *vs.* Y curves were found to be sharp (see figure 6). The position of the minimum changes with Z_0 and tends to $Y = -2$ as $Z_0 \to 1$, i.e. as the sphere moves closer and closer to the solid plate. It can also be seen from figure 6 that, for $Z_0 \lesssim 2$, after the

encounter all sphere trajectories are identical, independent of the initial separation distance Z_0.

It is of interest to note the interplay between sphere–wall and sphere–sphere interactions. For initial conditions near the wall, when the mobile sphere is far from the fixed one, the velocity of the sphere $U < 1$ owing to hydrodynamic sphere–wall resistance. When the sphere approaches the fixed sphere, sphere–sphere hydrodynamic interactions become noticeable on the background of the sphere–wall interactions. As a result of sphere–sphere interactions the moving sphere is pushed away from the wall when $Y \rightarrow 0$ (figures 3 and 4). The moving sphere is at the farthest distance from the wall when $Y = 0$. At this position sphere–wall interaction is minimum, while the sphere–sphere interaction reaches a maximum level. In the case of ideal smooth spheres the gap ϵ between spheres reaches its minimum value when $Y = 0$. For $Y > 0$ the process is reversed and the sphere trajectory is symmetrical with respect to the equatorial plane ($Y = 0$) of the deposited sphere. Such symmetrical trajectories were observed in our system for initial separation distances $Z_0 \geqslant 2.34$ (cf. figure 5).

The asymmetrical trajectories that we observe when $Z_0 \leqslant 2.0$ (figure 6) indicate that in our system the spheres were prevented from approaching to distances dictated by purely hydrodynamic considerations for ideal spheres. The fact that for initial wall separations $Z_0 \leqslant 2.3$ all the receding trajectories are identical suggests that the spheres are unable to approach closer than a certain distance, most likely determined by the surface roughness of the spheres. Here one is reminded of two-sphere trajectories in a simple shear flow, studied by Arp & Mason (1977*b*). For trajectory constants below a certain value, all receding trajectories were found to be identical. The minimum distance of approach determined from the receding trajectory was typical of the dimensions of the surface roughness of the spheres.

When $Z_0 \leqslant 2$ the experimentally determined sphere velocity at $Y = 0$ was $U_{\phi=0} = 0.49$ in all cases (figure 6), corresponding, according to (11), to $\epsilon = 4.2 \times 10^{-5}$ or to a gap width between the sphere in the absence of the wall of 0.13 μm. This gap width would be the minimum of approach if one sphere was fixed and the second moved in an unbounded liquid. The presence of a wall will decrease the sphere velocity. Thus, the velocity $U_{\phi=0} = 0.49$ in the presence of the wall indicates that in our system the minimum gap between spheres at $Y = 0$ was larger than 0.13 μm.

A second estimate can be made in a similar way from the velocity of the first more or less symmetrical trajectory (figure 5). For this trajectory $U_{\phi=0} = 0.54$, from which it follows that the gap width is about 1.6 μm. As a result of the presence of a wall the gap width of 1.6 μm cannot be considered as an upper limit, but rather as an approximate value showing order of magnitude of the maximum spheres roughness. Thus, we can conclude that the spheres roughness was larger than 0.13 μm and could be as large as a few micrometres.

Other possible factors contributing to asymmetrical trajectories are deviations from sphericity for one or both particles and specific properties of the thin liquid film in the gap. The deviation from sphericity of our spheres was less than 0.2 % and this will introduce only a very slight asymmetry in the trajectories (cf. Adamczyk & van de Ven 1983). Changes in properties of the liquid in a thin layer only manifest themselves for films thinner than 0.1 μm (Vrij 1966), which is smaller than the minimum distance of approach. Thus surface roughness is by far the most important factor causing the observed asymmetric trajectories.

The correctness of this conclusion is also confirmed by a scanning electron micrograph of the surface of the mobile sphere presented in figure 7. It can be seen

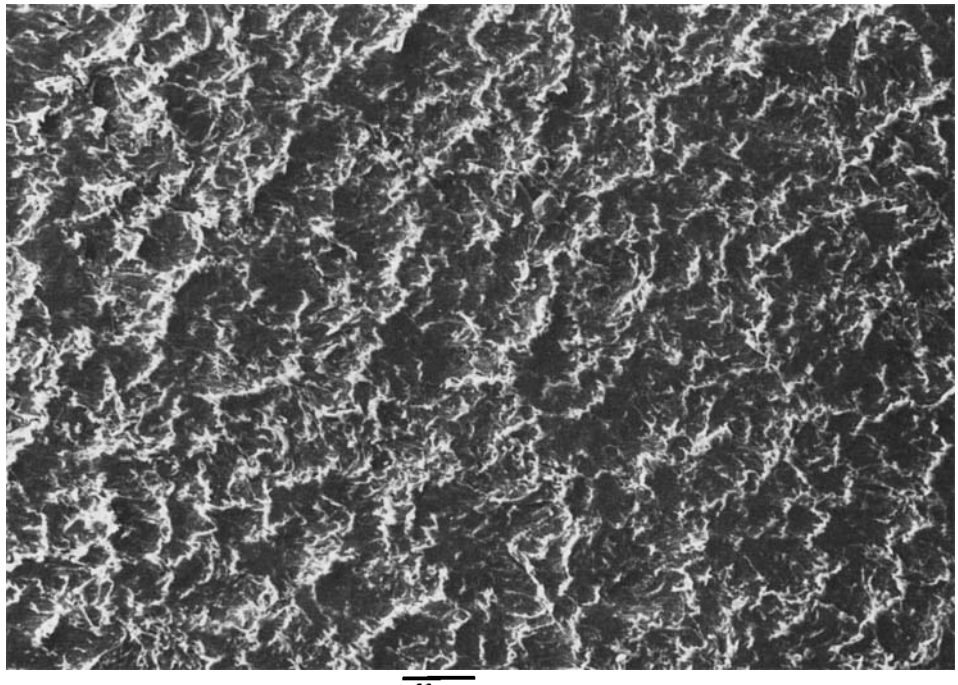

FIGURE 7. Scanning electron micrograph of the sphere surface.

that the surface of the sphere is not smooth. It is not possible to determine from this figure the depth of the surface rugosities, but the observed textures with a length-scale of 10 μm or more suggest a roughness of the order of a few micrometres. Thus the precision spheres used in our experiments had rather rough surfaces.

In figures 5 and 6 the full lines represent the theoretical velocity values calculated by the singularity method. The experimentally determined values of the distances Y and Z were used in the calculation of the theoretical values of the velocity at a given sphere position. For $Z_0 > 2$ (figure 5), a very good agreement between experimental and theoretical velocity values was found when $|Y| \geqslant 2.5$. When the sphere was closer to the wall, $1.05 < Z_0 \leqslant 2$ (figure 6), good agreement was obtained for $|Y| \geqslant 3.0$. For $Z_0 \lesssim 1.05$, theoretical predictions are inaccurate. Near the attached particle, i.e. for $-2.5 < Y < 2.5$, the good agreement between experiment and theory is only found when $Z_0 \geqslant 2.88$ (see figure 8). When $Z_0 = 2.88$ the results computed by the singularity method differ by 3% from the experimental data in the region $-2.5 < Y < 2.5$. These differences become more and more pronounced when the mobile sphere passes closer and closer to the fixed one, i.e. when Z_0 decreases. In principle it is possible to obtain better agreement by using more singular forces and sources in the numerical computations (at the cost of increased computer time).

The dependence of the experimentally determined sphere velocity on initial separation distance is shown in figure 9 for regions near to (lower curve) and far from (upper curve) the attached sphere. It can be seen from figure 9 that the fixed particle affected the motion of the moving one at separation distances smaller than 4.9. In this region the sphere velocities far from the centre of the attached particle (upper curve) were higher than the mobilities near the attached particle (lower curve). When

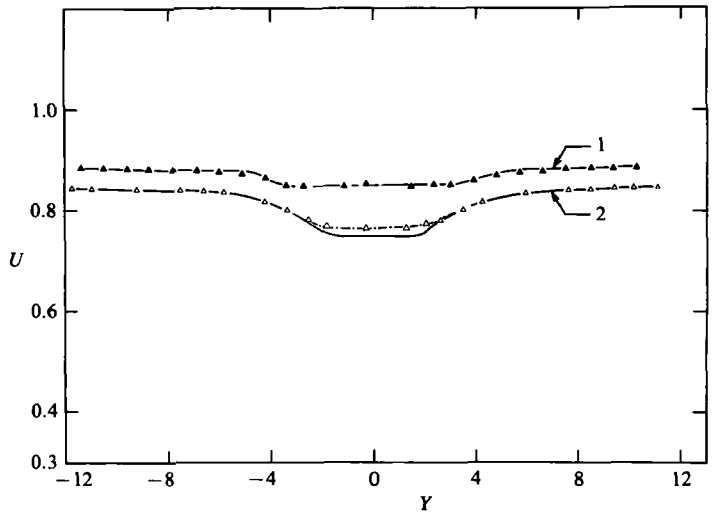

FIGURE 8. Comparison of the experimental and theoretical results for the region near the fixed sphere. Solid lines, experimental data for $Z_0 = 3.55$ (curve 1), and $Z_0 = 2.88$ (curve 2). Triangles are points calculated from the singularity method.

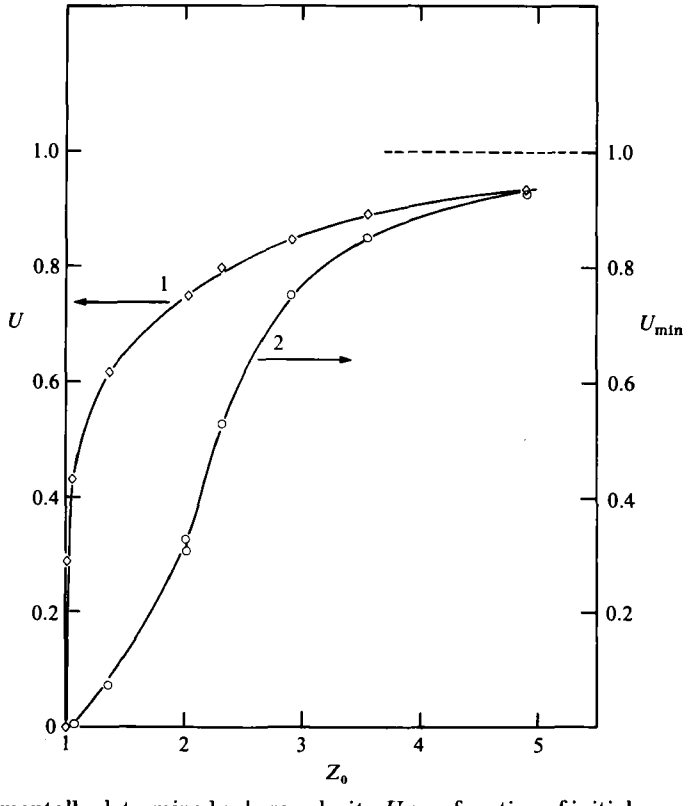

FIGURE 9. Experimentally determined sphere velocity U as a function of initial separation distance Z_0. Curve 1, velocity values for $Y < -8$. Curve 2, minimum values of the velocity in U *vs.* Y curves.

$Z_0 \geqslant 4.9$ the sphere–sphere hydrodynamic interactions were not detectable on the background of plate–sphere interactions.

5. Concluding remarks

Although theory predicts hydrodynamic two-sphere interactions to be symmetrical, for small initial wall–sphere separations actual trajectories were found to be asymmetric. We concluded that surface roughness prevents the spheres from approaching to within the small distances dictated by purely hydrodynamic considerations for ideal smooth spheres. For our spheres, roughness asperities of the order of micrometres were responsible for the asymmetric behaviour, observed for initial sphere–wall separations $Z_0 \lesssim 2$. For $Z_0 \geqslant 2.3$ the trajectories were found to be symmetrical and, when the distances between the mobile sphere and the fixed sphere were not too small, i.e. when $|Y| > 2.5$, the experimental observations agreed very well with the numerical calculations. For $Z_0 \gtrsim 2.9$, the singularity method is in fair agreement with experiment for all gap widths; for $Z_0 < 2.9$ discrepancies between theoretical predictions and experimental data become more and more pronounced when the mobile sphere is close to the fixed one. For $Z_0 \gtrsim 4.9$, sphere–sphere interactions are insignificant and undetectable on the background of sphere–wall interactions.

It is of interest to discuss what happens to spheres of colloidal size, i.e. in the range 10–1000 nm. In the absence of colloidal forces a surfaces roughness of 10^{-4} particle radius (a fraction of an ångstrom) will have a similar effect on the trajectory in pushing the mobile sphere away from the wall as in our macroscopic experiments. However other effects usually become important, such as van der Waals, electrostatic and possibly solvation forces. In an electrostatically stabilized suspension the energy of interaction between two particles exhibits an energy barrier at a distance h_b of a few nanometres, preventing closer contact. Assuming $h_b \approx 3$ nm, then $\epsilon_m \approx 0.3$–0.003 (for $a = 10$–1000 nm). This corresponds to $U_{\phi=0}$ ranging from 0.6 to 0.8 (cf. equation 11), which in turn corresponds to distances to the wall (after the encounter) in the range $Z = 2.5$–3.2. This means that, when a mobile colloidal particle encounters a similar particle deposited on a wall, it will be pushed a substantial distance away from the wall. The probability that the mobile particle will deposit on the wall is thereby considerably reduced. Such phenomena appear to be responsible for blocking effects occurring in coating processes. To understand these phenomena in a more quantitative way, more accurate predictions of hydrodynamic two-sphere interactions at a wall are needed, especially for small gap widths.

REFERENCES

Adamczyk, Z. & van de Ven, T. G. M. 1983 Pathlines around freely rotating spheroids in simple shear flow. *Intl J. Multiphase Flow* **9**, 203.

Adamczyk, Z., Adamczyk, M. & van de Ven, T. G. M. 1983 Resistance coefficient of a solid sphere approaching plane and curved boundaries. *J. Colloid Interface Sci.* **96**, 204.

Adler, P. M. 1981*a* Heterocoagulation in shear flow. *J. Colloid Interface Sci.* **83**, 106.

Adler, P. M. 1981*b* Interaction of unequal spheres. I. Hydrodynamic interaction: colloidal forces. *J. Colloid Interface Sci.* **84**, 461.

Ambari, A., Manuel, B. G. & Guyon, E. 1983 Effect of a plane wall on a sphere moving parallel to it. *J. Physique Lettres* **44**, L-143.

Arp, P. A. & Mason, S. G. 1977*a* The kinetics of flowing dispersions. VIII. Doublets of rigid spheres (theoretical). *J. Colloid Interface Sci.* **61**, 21.

ARP, P. A. & MASON, S. G. 1977*b* The kinetics of flowing dispersions. XI. Doublets of rigid spheres (experimental). *J. Colloid Interface Sci.* **61**, 44.

BATCHELOR, G. K. & GREEN, J. T. 1972 The hydrodynamic interaction of two small freely-moving spheres in a linear flow field. *J. Fluid Mech.* **56**, 375.

BLAKE, J. R. 1971 A note on the image system for a Stokeslet in a no-slip boundary. *Proc. Camb. Phil. Soc.* **70**, 303.

BLAKE, J. R. & CHWANG, A. T. 1974 Fundamental singularities of viscous flow. Part 1: The image system in the vicinity of a stationary no-slip boundary. *J. Eng. Math.* **8**, 23.

COX, R. G. & MASON, S. G. 1971 Suspended particles in fluid flow through tubes. *Ann. Rev. Fluid Mech.* **3**, 191.

DĄBROŚ, T. & VAN DE VEN, T. G. M. 1982 Kinetics of coating by colloidal particles. *J. Colloid Interface Sci.* **89**, 232.

DĄBROŚ, T. & VAN DE VEN, T. G. M. 1983 On the effects of blocking and particle detachment on coating kinetics. *J. Colloid Interface Sci.* **93**, 576.

DĄBROŚ, T. 1985 A singularity method for calculating hydrodynamic forces and particle velocities in low Reynolds number flows. *J. Fluid Mech.* **156**, 1.

DARABANER, C. L. & MASON, S. G. 1967 Particle motion in sheared suspensions. XXII. Interactions of rigid spheres (experimental). *Rheol. Acta* **6**, 273.

DAVIS, M. H. 1969 The slow translation and rotation of two unequal spheres in a viscous flow. *Chem. Engng Sci.* **24**, 1769.

FAXEN, H. 1923 Die Bewegung einer starren Kugel längs der Achse eines mit zäher Flüssigkeit gefüllten Rohres. *Ark. Mat. Astron. Fys.* **17**, 1.

GOLDMAN, A. J., COX, R. G. & BRENNER, H. 1967 Slow viscous motion of a sphere parallel to a plane wall. I. Motion through a quiescent liquid. *Chem. Engng Sci.* **22**, 637.

JEFFREY, D. J. & ONISHI, Y. 1984 Calculation of the resistance and mobility functions for two unequal rigid spheres in low-Reynolds-number flow. *J. Fluid Mech.* **139**, 261.

MAUDE, A. D. 1961 End effects in a falling-sphere viscometer. *Brit. J. Appl. Phys.* **12**, 293.

MIYAMURA, A., JWASAKI, S. & ISHII, T. 1981 Experimental wall correction factors of single solid spheres in triangular and square cylinders, and parallel plates. *Intl J. Multiphase Flow* **7**, 41.

O'NEILL, M. E. 1968 A sphere in contact with a plane wall in a slow linear shear flow. *Chem. Engng Sci.* **23**, 1923.

O'NEILL, M. E. & STEWARTSON, K. 1967 On the slow motion of a sphere parallel to a nearby parallel wall. *J. Fluid Mech.* **27**, 705.

O'NEILL, M. E. & MAJUMDAR, S. R. 1970 Asymmetrical slow viscous fluid motions caused by the translation or rotation of two spheres. Part I. The determination of exact solutions for any values of the ratio of radii and separation parameters. *Z. angew. Math.* **21**, 164.

STIMSON, M. & JEFFERY, G. B. 1926 The motion of two spheres in a viscous fluid. *Proc. R. Soc. Lond.* A **111**, 110.

TAKAMURA, K., GOLDSMITH, H. L. & MASON, S. G. 1981 The microrheology of colloidal dispersions. XII. Trajectories of orthokinetic pair-collisions of latex spheres in a simple electrolyte. *J. Colloid Interface Sci.* **82**, 175.

VAN DE VEN, T. G. M. & MASON, S. G. 1976 The microrheology of colloidal dispersions. IV. Pairs of interacting spheres in shear flow. *J. Colloid Interface Sci.* **57**, 505.

VAN DE VEN, T. G. M. & MASON, S. G. 1977 The microrheology of colloidal dispersions. VII. Orthokinetic doublet formation of spheres. *Coll. Polymer Sci.* **255**, 794.

VAN DE VEN, T. G. M. 1982 Interactions between colloidal particles in simple shear flow. *Adv. Colloid Interface Sci.* **17**, 105.

VRIJ, A. 1966 Possible mechanism for the spontaneous rupture of thin, free liquid films. *Trans. Faraday Soc.* **42**, 23.